COMPONENTS' AND MATERIALS' PERFORMANCE FOR ADVANCED SOLAR SUPERCRITICAL CO2 POWERPLANTS

Process Parameters of Solar Particle Cycle

Deliverable 1.2

WP1: Materials operation conditions and their feasibility studies

Date: March 24th 2022

Deliverable type: Report

Dissemination level: Public

Lead participant: DLR

This project has received funding from the European Union's Horizon 2020 Research and Innovation Action (RIA) under grant agreement No. **958418.**

AUTHORS

Name	Organization
Lukas Heller	DLR
Maxime Rouzes	John Cockerill
Hicham Barbri	DLR
Daniel Benitez	DLR
Reiner Buck	DLR

DOCUMENT HISTORY

Version	Date	Change
01	31/01/2021	Initial version uploaded
02	24/03/2022	Heat exchanger design reviewed (Sections 3.2, 3.3 and 3.4)

ABOUT THE PROJECT

COMPASsCO_2 is a 4-year HORIZON2020 project started on 1.11.2020. It is led by the German Aerospace Center (DLR), with eleven additional partners from seven European countries.

COMPASsCO_2 aims to integrate CSP particle systems into highly efficient sCO_2 Brayton power cycles for electricity production. In COMPASsCO2, the key component for such an integration, i.e. the particle-sCO_2 heat exchanger, will be validated in a relevant environment. To reach this goal, the consortium will produce tailored particle and alloy combinations that meet the extreme operating conditions in terms of temperature, pressure, abrasion and hot oxidation/carburization of the heat exchanger tubes and the particles moving around/across them. The proposed innovative CSP sCO_2 Brayton cycle plants will be flexible, highly efficient, economic and 100% carbon neutral large-scale electricity producers.

The research focus of COMPASsCO2 is on three main technological improvements: development of new particles, development of new metal alloys and development of the heat exchanger section.

DISCLAIMER

This project has received funding from the European Union's Horizon 2020 Research and Innovation Action (RIA) under grant agreement No. **958418.**

Table of Contents

LIST OF FIGURES

LIST OF TABLES

LIST OF ABBREVIATIONS

CSP	Concentrating Solar Power
EC	European Commission
EU	European Union
HX	Heat exchanger
PHX	Primary heat exchanger
LMTD	the logarithmic-mean temperature difference
sCO_2	Supercritical carbon dioxide
ASME	American Society of mechanical Engineers
LCOE	Levelized cost of electricity
DLR	Deutsches Zentrum für Luft- und Raumfahrt e.V.
MAS	Maximum allowable stress
TES	Thermal energy storage

1 ABSTRACT

Work Package 1 of COMPASsCO2 is mainly focused on material operating conditions in an industrial environment and is divided into different tasks. This report concerns its second task, which is dedicated to the solar particle cycle including the particle- sCO_2 heat exchanger.

Deliverable 1.1 from this work package allowed us to define the process parameters of the two heat exchangers (a high pressure and a low pressure) for the particles and supercritical CO_2. Based on that information, two particle- sCO_2 tubular heat exchangers were designed. The heat exchangers' design consists in several bundles of horizontal tubes heated by a hot falling bed of bauxite particles. Four different alloys were assessed for the heat exchangers composition among which only two were able to withstand the high pressure and temperature encountered. These two alloys are Haynes 282 and Alloy 740.

For the given sCO_2 power block and heat exchanger, a solar particle system based on the CentRec® receiver technology was defined. This mainly comprises the heliostat field layout, the receiver geometry and the thermal energy storage system sizing. The DLR's software HFLCAL was used to determine parameters that define these subsystems, namely, the number and position of heliostats, receiver aperture area, tower height, particle temperatures and particle inventory. Furthermore, the heliostat field and the receiver design efficiency, respectively, was estimated for the design point and as an annual average. Additional relevant parameters for high-temperature component and particle development are discussed.

2 INTRODUCTION

The aim of this deliverable is to determine the operating conditions in the particle cycle, defined by the particle- sCO_2 heat exchanger (HX), the solar field, the receiver and the thermal energy storage (TES) system. The first part of this deliverable, therefore, concerns the development of a concept design of the particle- sCO_2 heat exchanger. The second part describes the preliminary design of the heliostat field layout, receiver geometry and TES system parameters. The schematic of the overall system is depicted in Figure 1; it should be mentioned that the sCO_2 cycle shown is not corresponding to the cycle selected and presented in Deliverable 1.1, this figure is only to illustrate the relationship between the solar plant and the power block.

A description and selection of the sCO_2 Brayton cycle has been provided in COMPASsCO2 Deliverable 1.1 "Process parameters of solar sCO_2 Brayton cycle".

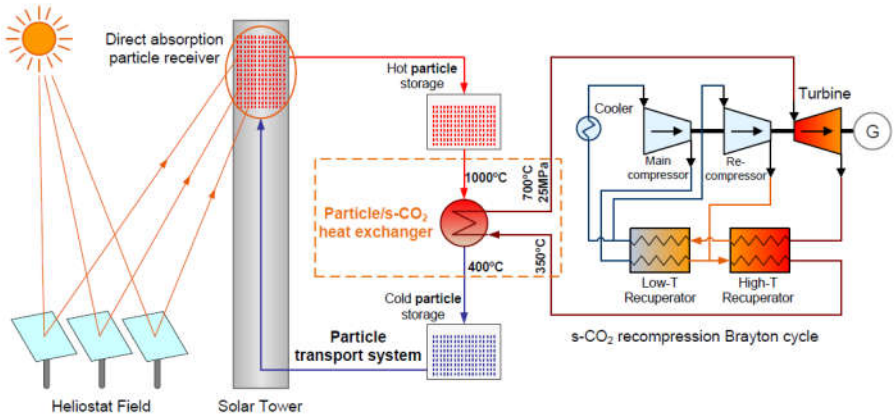

Figure 1: Schematic of a Particle-sCO2 CSP plant.

2.1 Particle-sCO_2 Heat Exchanger

The particle-sCO_2 heat exchanger concept is characterized by a moving bulk of particles that flows top-down through bundles of horizontal tubes. The sCO_2 at high pressure circulates through the tubes and is heated up by the hot particle flow. As the particles at the heat exchanger inlet reach 900°C, it is important to select noble alloys that can withstand this high temperature and also the daily thermal gradient during the start-up and shut down of the plant. In addition to the high temperature and pressure levels, the materials of the heat exchanger are exposed to erosion from the particle side and corrosion and oxidation from the sCO_2 side.

2.2 Solar Particle Loop

The solar particle loop provides and stores the thermal energy needed to power the particle-sCO_2 HX and, therefore, to the power block. It consists of the heliostat field, a thermal receiver on top of a tower, a vertical particle transport system and the thermal energy storage (TES) system. Depending on the size of the plant and the employed receiver technology, several heliostat fields, towers and receivers can be combined to feed a single heat exchanger and power block. The TES system can then either be decentralized, with hot and cold storage tanks at each tower, or be located as a single system close to the power block.

Within the COMPASsCO2 Project, a centrifugal particle receiver, based on the CentRec® Technology (Wu, Amsbeck et al. 2014), is employed. This technology is based on a rotating drum covered by a thin layer of small particles on the inside (see Figure 2). This layer is directly irradiated with highly concentrated sunlight through the aperture opening of the drum. By adjusting the rotational speed of the drum, the retention time of particles in the receiver can be adjusted to achieve the desired outlet temperature. A prototype CentRec® Receiver has achieved particle outlet temperatures of more than 950 °C (Ebert, Amsbeck et al. 2019).

These high outlet temperatures would result in high losses in an external receiver. A cavity receiver, as is the CentRec®, can achieve much higher efficiencies but requires a high solar flux at its cavity, which can only be achieved with a polar field. As polar fields are more limited in size than surrounding fields, commercial size CSP plants employing the CentRec® technology will most likely be multi-tower configurations.

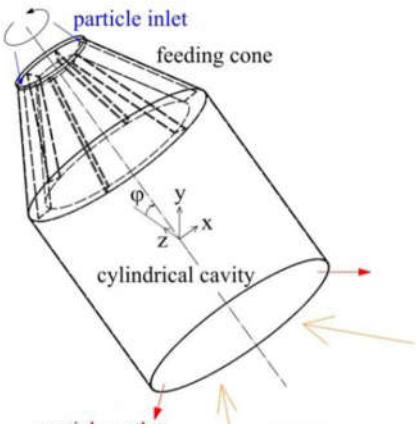

Figure 2: Principle design of the Centrifugal Particle Receiver (Wu, Amsbeck et al. 2014)

Besides the receiver and the heat exchanger, the particle loop consists of vertical and horizontal (at least in the case of multi-tower configurations) transport systems and the TES system. The latter is foreseen as several insulated tanks. For the vertical transport of particles,

several options are conceivable, depending on tower height and required mass flow. The horizontal transport has been proposed to be conducted by (autonomous) trucks (Buck and Giuliano 2018). The parasitic consumption for both transport systems is expected to be lower than in state of the art CSP plants with molten salt as the heat transfer medium.

The detailed design of the solar particle loop is not in the scope of COMPASsCO2, as the components mentioned above are either on high TRL already (such as the receiver), or are being developed in other projects (such as the particle transport systems of decentralized tower systems). In this document the selection of the components is done in order to define the boundary conditions that affect the particle-sCO_2 HX on the particle side.

3 HEAT EXCHANGER CONCEPT DESIGN

3.1 Heat exchanger concept

The heat exchanger design is made up of several bundles of tubes through which the sCO_2 flows. A moving bulk, composed of bauxite particles, flows top-down across the tubes bundles while heating them up. The concept of the heat exchanger is illustrated in Figure 3.

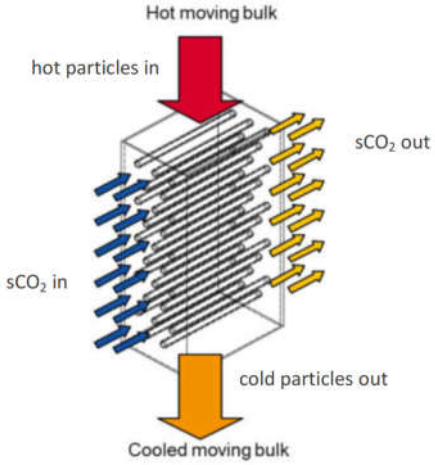

Figure 3: Heat exchanger concept [derived from (Buck and Giuliano 2018) based on (Baumann and Zunft 2015)]

3.2 Process parameters and technical limitations

As described in Deliverable 1.1, the selection of a Supercritical Partial Cooling cycle with Intercooling and Reheating lead to defining the process parameters values. Such a cycle requires two heat exchangers comprising both high- and low-pressure related sections. For the sake of clarity, the process parameters are shown below in Figure 4.

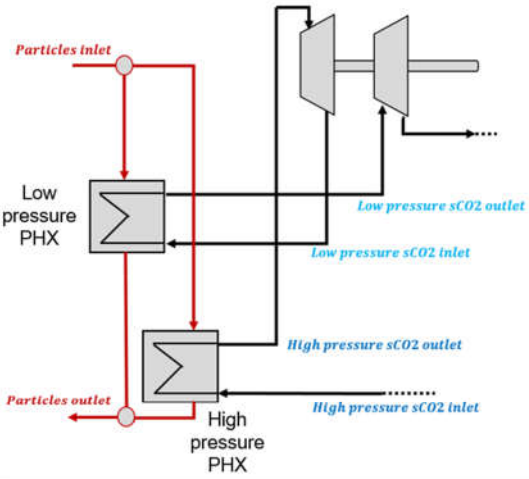

Parameters	Particles (high pressure PHX)	Particles (Low pressure PHX)	sCO2 (high pressure PHX)	sCO2 (low pressure PHX)
PHX inlet temperature [°C]	900	900	532.8	583.4
PHX outlet temperature [°C]	582.8	633.4	700	700
PHX inlet pressure [bar]	/	/	265.3	110.4
PHX outlet pressure [bar]	/	/	260	108.2
Mass flowrate [kg/s]	355.9	288.3	632.6	632.6

Figure 4: Process parameters of both high- and low-pressure heat exchangers

These values are the result of a basic design carried out using the Engineering Equation Solver software (EES). The underlying model is based on the logarithmic-mean temperature difference (LMTD) coupled with enthalpy balances both on particle and sCO2 sides.

Regarding the thermodynamic modelling, the inputs are:

- PHX process parameters
- Pressure drop = 5 bar

The thermal aspects of the design refer to both particle and sCO2 heat transfer coefficients.

The external heat transfer coefficient on the particle side was computed from simulations assuming a fixed heat exchanger geometrical arrangement (horizontal and vertical tube pitches, tube diameter and thickness). It was provided by project partner (DLR) and equal to an average of 200 W/(m².K) at first approximation in the EES model.

The sCO2 heat transfer coefficient was assessed using the Jackson correlation giving a Nusselt number as a function of both Reynolds and Prandtl numbers. This correlation was chosen over the usual Gnielinski correlation as it appears giving better results for supercritical fluids. It accounts for the radial density variation distribution within the pipe and gives conservative results regarding assessment of metal temperature compared to Gnielinski correlation.

$$Nu = 0.0183 Re_b^{0.82} \overline{Pr^{0.5}} \left(\frac{\rho_w}{\rho_b}\right)^{0.3}$$

Where:

- Re: Reynolds number
- Pr: Prandtl number assessed at a temperature equal to (Tb+Tw)/2
- Subscripts b and w refer to bulk and wall respectively.

The assessed sCO2 heat transfer coefficient was found being strongly constrained by the imposed pressure drop over the whole heat exchanger. Pressure drop is around 2% of the design pressure, which is a reasonable assumption. This heat transfer coefficient was found to be around 2500-3000 W/(m².K) with a corresponding velocity around 10 m/s. This is quite lower than what was anticipated (~10000 w/(m².K)) at the beginning of the project, and with a direct impact on the HX design as shown in section 3.4 below. The design of the HX is fully detailed in Deliverable 1.3 as well.

Finally, tube conduction resistance is also accounting for in the overall calculations as it has a non-negligible effect on the thermal behavior of the system.

3.3 Material selection

3.3.1 Selection of an alloy for the HX

Different alloys were considered within the framework of the project as shown in Table 1 below.

Table 1: Material selection based on the ASME code

Alloy denomination	Verification with the ASME VIII division 1 (2019 version)
Sanicro 25	MAS too low
Alloy 617	MAS too low
Alloy 740	MAS high enough
Haynes 282	MAS high enough

For both low- and high-pressure HX, each alloy was evaluated at the expected design pressure and temperature according to the ASME VIII division 1 code. At the design temperature of 760°C, two of the alloys showed too low Maximum Allowable Stress (MAS) values to withstand the operating conditions: Sanicro 25 and alloy 617.

Alloy 740H and Haynes 282 satisfied the ASME code under the harsh occurring conditions within the HX. The material selection for the HXs will be further discussed in the section 3.4. Details can also be found in Deliverable 1.3.

3.3.2 Selection of the type of particles

State-of-the-art particles considered for the design are bauxite particles that are intermediate strength proppants. These particles are engineered to deliver superior conductivity and are characterized by a specific heat of 1200 J/(kg.K). Two particle mean diameters were considered: 450µm and 900 µm. A literature review was carried out and detailed in Deliverable 1.3.

3.4 Heat exchanger design

The process parameters and heat exchanger design led to one design for the high-pressure heat exchanger and a slightly different one for the low-pressure heat exchanger.

Both low- and high-pressure heat exchangers were confronted to two different inlet particle velocities: 1 mm/s and 2.5 mm/s. Particle diameter does not influence the HX geometrical dimensions.

For the sake of comparison, both low- and high-pressure heat exchanger designs are compared in Table 2 for the same alloy Haynes 282. An in-depth analysis was carried out to validate the state-of-the-art materials of the HX. This analysis involves calculating the thermomechanical stress coupled with an assessment of the stress-rupture time. It is fully detailed in Deliverable 1.3, section 4. It shows that Inconel 740H cannot be considered for the high-pressure HX but remains a good candidate for the low-pressure HX.

However, at this stage of the design, these results must be considered as trends more than definite conclusions. Indeed, the choice between designs would require a more detailed analysis usually carried out in detailed engineering, which is not within the scope of the project. Open questions remain for instance regarding the influence of the change in vertical pitch on particle heat transfer coefficient. This choice must be done accounting for the possible manufactured bending radius and its influence on particle heat transfer.

Since the most detrimental conditions occur in the high-pressure HX and considering the results from the analysis, the chosen HX design refers to the lowest inlet particle velocity. The drawing in Figure 5 uses therefore the appropriate parameters shown in Table 2.

Both alloys 740H and 282 are good candidates for the low-pressure heat exchanger regardless of the inlet particle velocity. The choice can therefore be done on which one gives the best heat exchange. The latter occurs with the highest inlet particle velocity of 2.5 mm/s. It is this design which is considered for the low-pressure heat exchanger.

Finally, both low- and high-pressure chosen heat exchanger design parameters are set to bold characters (see Table 2**)**.

Table 2: low- and high-pressure heat exchanger design parameters for both inlet particle velocities 1 mm/s and 2.5 mm/s and Haynes 282.

Design parameter	Unit	High-pressure PHX		Low-pressure HX	
		V_{part} = 1 mm/s	V_{part} = 2.5 mm/s	V_{part} = 1 mm/s	V_{part} = 2.5 mm/s
Arrangement	**[-]**	**Staggered**	Staggered	Staggered	**Staggered**
Tube external diameter	**mm**	**60.3**	60.3	60.3	**60.3**
Tube wall thickness	**mm**	**8.7**	8.7	4.4	**4.4**
Number of elements	**[-]**	**334**	334	281	**281**
Tube length per row	**m**	**7.8**	3.1	9.2	**3.6**
Number of rows	**[-]**	**20**	48	14	**32**
Number of tubes carrying flow	**[-]**	**1**	1	1	**1**
Horizontal pitch	**mm**	**17.4**	17.4	17.4	**17.4**

between tubes					
Vertical pitch between	mm	9	9	9	9
Total HX horizontal width	m	23.2	23.2	19.5	19.5
Total HX vertical height	m	1.5	3.8	1.1	2.5

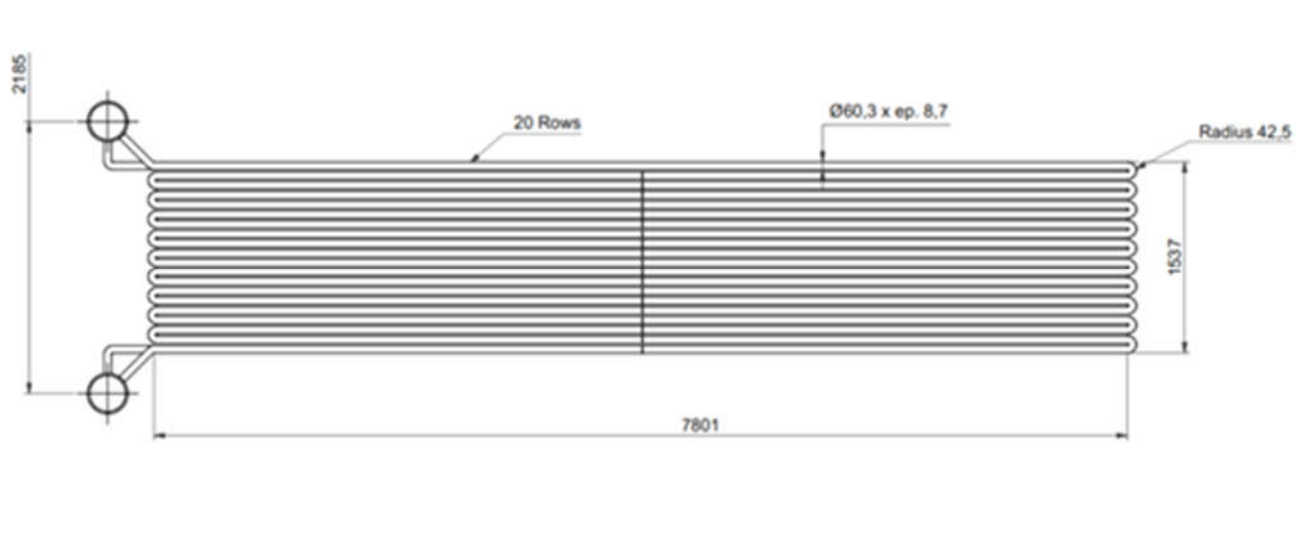

Figure 5: isometrical view of the high-pressure heat exchanger for inlet particle velocity 1 mm/s and particle diameter of 450 µm.

4 PRELIMINARY SOLAR FIELD DESIGN

The developed solar field design consists of several towers containing a single CentRec® receiver each and with an associated field of heliostats. The heated particles are transported from the towers to a central power block and returned at cold tank temperatures. In the following, such a plant is optimized using the DLR tool Visual HFLCAL (Schwarzbözl, Pitz-Paal et al. 2009) in Version 13 Beta.

4.1 Input Parameters

Certain parameters have to be defined a priori. For example, the size of the solar power plant is derived from currently developed commercial tower plants, as is its location. Receiver-related parameters are based on DLR-internal experience with the CentRec® technology and CSP plants in general. Particle temperatures at the HX are derived from its concept design (See Section 3). A list of all input parameters to the HFLCAL Model can be found in Annex 1, the most important ones are additionally presented in Table 3.

Table 3: Main input parameters to field optimization (dp: design point)

Parameter	Value	Comment [Source]
Location	Postmasburg, RSA	Location of Redstone Solar Thermal Power Plant Project

Power block net rating	**112.8 MW_e**	**Based on cycle chosen in Deliverable 1.1**
Mean receiver outlet temperature @ dp	**905 °C**	**Sufficient to reach particle inlet temperature to the HX (900 °C)**
Max. particle temperature	**~1000 °C**	**Due to inhomogeneous temperature distribution**
Receiver inlet temperature @ dp	**605.5 °C**	**Derived from HX design**
Receiver thermal power @ dp	**96.23 MW_t**	**Per unit**
Number of towers and receivers	**6**	
Solar multiple	**2.5**	**Oversizing of solar field relative to power plant design point thermal demand**
Thermal storage capacity	**12 h**	**hours of discharging at full load**

4.2 Methodology

The heliostat field layout was optimized by minimizing the estimated LCOE of the system. This requires three steps: (a) calculation of the annual thermal output of the receiver system, (b) determination of the capital and operational expenditure of the plant and, finally, (c) variation of parameters defining the number of heliostats in the field, their position and of the receiver system. All of these steps were done within the Visual HFLCAL software. While Steps (a) and (c) are part of the standard distribution of the software (Schwarzbözl, Pitz-Paal et al. 2009), cost and efficiency data for the TES system and power block had to be implemented as special routines.

The subsystem cost models are based on typical values for standard CSP systems (e.g., the heliostat field), DLR-internal assumptions for particle-related systems and the estimated cost for the chosen sCO_2 power block (see Deliverable 1.1 and Heller, Glos et al. in press). The chosen values are furthermore listed in Annex 1.

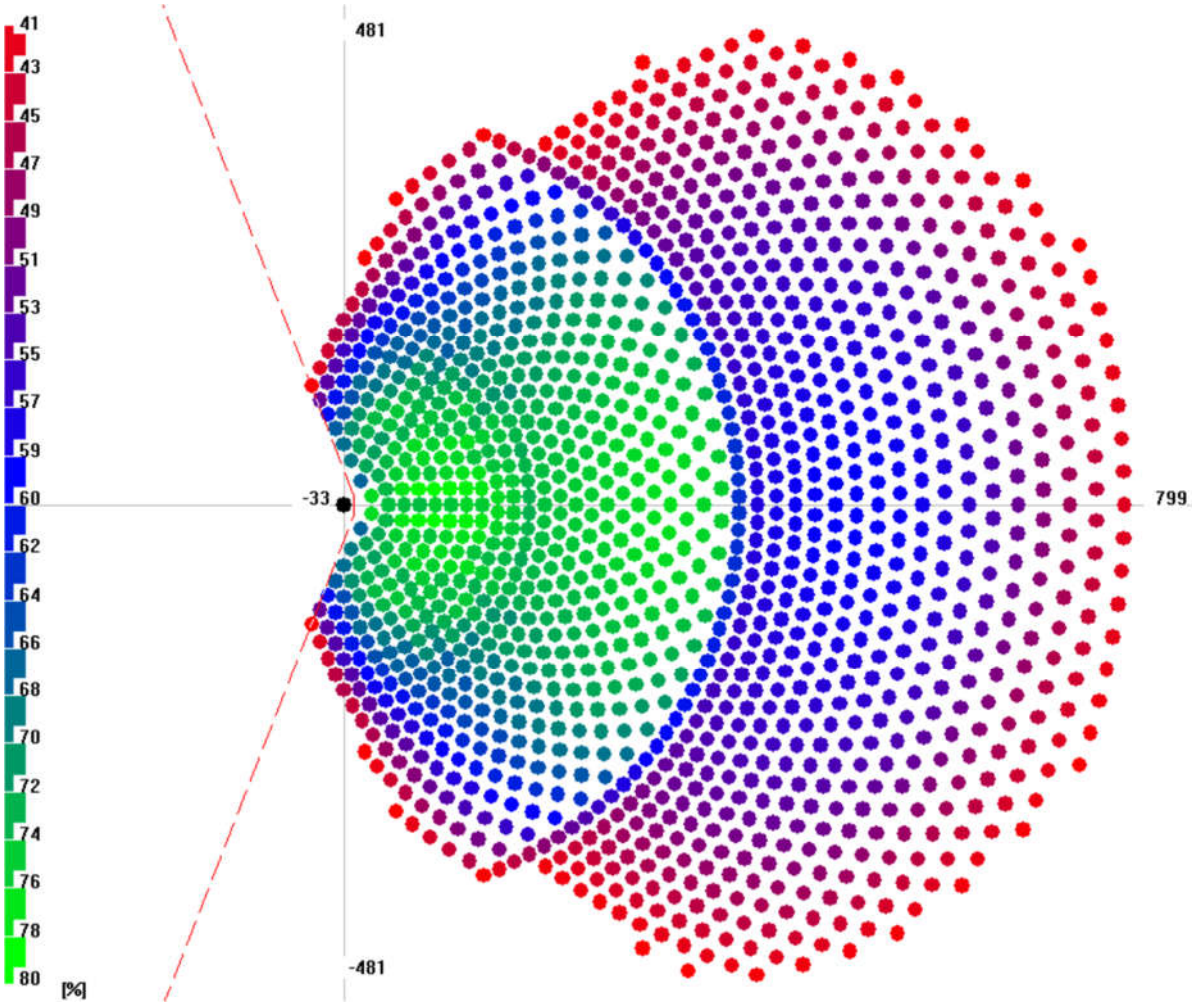

Figure 6: Heliostat field layout showing average annual efficiency per heliostat (color code)

4.3 Optimization Results

The heliostat field layout with the minimum levelized cost of electricity (LCOE) as derived by HFLCAL is depicted in Figure 7. The major results are presented in Table 4 and further details are given in Annex 1. These results are in the expected range for a large cavity receiver system. The very high flux at the aperture of the receiver leads to a high thermal efficiency (considering the high outlet temperature) while the optical efficiency of the field is penalized.

Table 4: Main results of field optimization (dp: design point)

Parameter	Unit	Value
Height of receiver center above ground	[m]	133.6
Receiver aperture diameter	[m]	7.58
Mean solar flux at receiver aperture @ dp	[MW/m^2]	2.38
Heliostat aperture area (per tower)	[m^2]	170 000
Particle inventory (per tower)	[t]	5172
Field efficiency @ dp	[-]	63.6 %
Field efficiency, annual average	[-]	54.2 %
Receiver efficiency @ dp	[-]	89.7 %
Receiver efficiency, annual average	[-]	87.4 %

The required particle inventory is determined by the thermal demand of the power block, the storage size and the temperature spread between hot and cold tank. Due to the high temperature of the sCO_2 at the inlet to the heat exchanger (~550 °C), this spread is only approximately 300 K in the investigated setup, leading in turn to a rather large particle inventory.

4.4 Additional Relevant Parameters

Some additional parameters, which don't follow directly from the heliostat field and receiver layout, could provide valuable information for material considerations. These are given in the following.

4.4.1 Solar Flux

The mean solar flux on the receiver aperture for the defined design is given in Table 3. The flux distribution on the particles on the receiver inner wall could be calculated for each time step/sun position via raytracing. However, as currently it is not foreseen that this data will be needed for the development tasks in the COMPASsCO2 Project, these raytracing simulations were not conducted at this point in time. In case this detailed information is needed, it can be provided upon request.

4.4.2 Thermal Shock During Cloud Transients or Shut Down

As part of the CENTREC500 project, in which a 500 kW_t receiver with an aperture diameter of 1.13 m was developed, the temperature drop at defocus was investigated. Figure 8 shows the measured temperatures in the receiver. The heliostat field was automatically defocused at a certain time and a temperature drop of around 20 °C/min was observed.

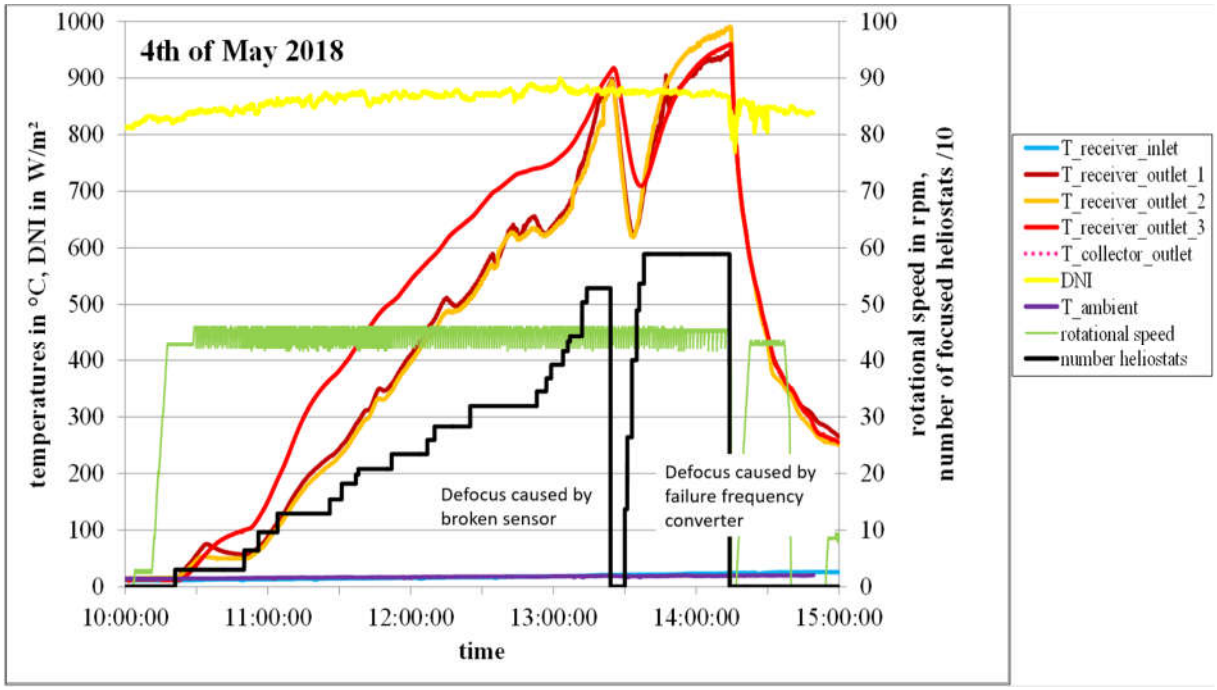

Figure 7 Temperature measurements in Centrec500 receiver

In addition, other projects, such as the HIFLEX project, and doctoral theses are being undertaken to investigate the behavior of the receiver in a transient state. More information about the transient behavior of the receiver will be provided later. For the scope of

COMPASsCO2 this effect seems not to be very relevant, as the large storage tank allows to near steady conditions at the PHX inlet on the particle side. For the particles themselves, it is to be investigated if strong temperature gradients at the receiver may affect them.

4.4.3 Particle Velocities in the Receiver

The velocity profile of the particles in the receiver depends on the thickness of the particle film. Numerical and experimental investigations have already been carried out in a small prototype for this purpose. For this investigation Bauxite particles from the company Saint Gobain with 1.2 mm Sauter diameter (mesh size 16/13) are employed. The rotational speed and inlet particle mass flow rate are 150 rpm and 25 g/s, respectively. Figure 8 shows the velocity profile in the axial direction of 13.8 cm aperture diameter receiver. It can be seen that the velocity profile of the particles has roughly exponential behavior. It means that the layer absorbing the solar rays, which are mostly the first two layers, have less residence time, while the shaded layers, which are mostly heated by conduction and short-range radiation, move more slowly.

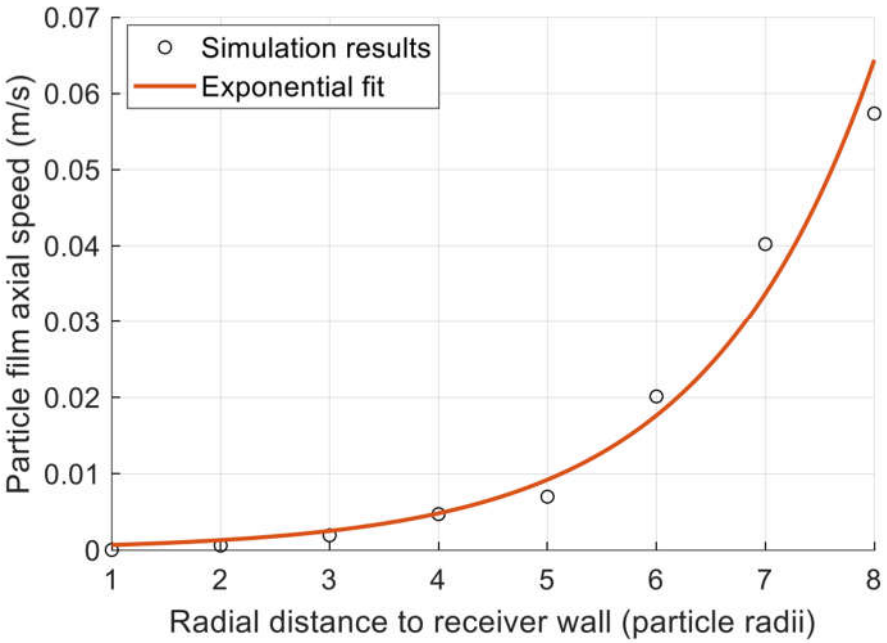

Figure 8 Velocity profile of particle film in radial direction

Due to the relatively high mass flow in COMPASsCO2, which is around 100 kg/s per receiver, the velocity profile shown above cannot be directly used because of the large difference in size. Since no experiences are available for such large mass flows, DLR is currently in the process of developing a model that determines the particle velocities for different mass flows as well as different rotation speeds. The model is estimated to be available in the middle of 2021, and only by then detailed information about the particle velocity can be provided.

4.4.4 Falling Distance from Receiver to Containment Vessel

The vertical distance between the receiver outlet and the containment vessel depends on specific tower designs. Furthermore, design measures to minimize the falling distance, e.g. by introducing inclined pipes, are conceivable. Therefore, a critical falling distance should rather be defined so that the necessity of and requirements on such measures can be evaluated.

5 BIBLIOGRAPHY

Balz, M., V. Göcke, T. Keck, F. v. Reeken, G. Weinrebe and M. Wöhrbach (2016). "Stellio – development, construction and testing of a smart heliostat." **1734**(1): 020002.

Baumann, T. and S. Zunft (2015). "Development and Performance Assessment of a Moving Bed Heat Exchanger for Solar Central Receiver Power Plants." Energy Procedia **69**: 748-757.

Buck, R. and S. Giuliano (2018). Impact of solar tower design parameters on sCO2-based solar tower plants. 2nd European sCO2 Conference 2018, Essen, Germany.

CORDIS. "HIgh storage density solar power plant for FLEXible energy systems." Retrieved 21. January, 2021, from https://cordis.europa.eu/project/id/857768.

Ebert, M., L. Amsbeck, J. Rheinländer, B. Schlögl-Knothe, S. Schmitz, M. Sibum, R. Uhlig and R. Buck (2019). "Operational experience of a centrifugal particle receiver prototype." **2126**(1): 030018.

Giuliano, S., M. Puppe, C. Frantz, R. Uhlig, R. Flesch, T. Baumann, S. Schmalz, D. Waldmann, Barbara, D. Storm, Christian, R. Schumacher, W. Ibraheem, M. Aust, M. Engelhard, D. Peter, C. Guder, M. Spiegel, C. Schwager, C. Teixeira Boura, S. Alexopoulos, H. Hattendorf, J. Wortmann, M. Hinrichs and M. Korte (2017). HPMS - High Performance Molten Salt Tower Receiver System.

Gnielinski, V. (2010). G1 Heat Transfer in Pipe Flow. VDI Heat Atlas. Berlin, Heidelberg, Springer Berlin Heidelberg**:** 691-700.

Heller, L., S. Glos and R. Buck (in press). SCO2 Power Cycle Design without Heat Source Limitations: Solar Thermal Particle Technologyin the CARBOSOLA Project. 4th European sCO2 Conference for Energy Systems, Prague, Czech Republic.

Schwarzbözl, P., R. Pitz-Paal and M. Schmitz (2009). Visual HFLCAL - A Software Tool for Layout and Optimisation of Heliostat Fields. SolarPACES 2009. T. Mancini and R. Pitz-Paal. Berlin.

Wu, W., L. Amsbeck, R. Buck, R. Uhlig and R. Ritz-Paal (2014). "Proof of Concept Test of a Centrifugal Particle Receiver." Energy Procedia **49**: 560-568.

S. Hicdurmaz, E. Johnson, J. Grobbel, L. Amsbeck, R. Buck, B. Hoffschmidt (2020). "Numerical Heat Transfer Modelling of a Centrifugal Solar Particle Receiver" SolarPACES 2020

6 ANNEXES

6.1 Annex 1. HFLCAL Databook

No.	Item	Unit	Value	Comments
	Location			
1.	Location name	[]	Postmasburg, South Africa	Location of Redstone Solar Thermal Power Plant Project
2.	Latitude	[°] N	-28.298	According to meteo file
3.	Longitude	[°] E	23.366	
4.	Altitude	[m]	1514	
5.	Annual DNI	[kW h/ (m^2 year)]	2657	
	Design Points			
6.	Design point	[tt:mm - hh]	21.03. – solar noon	
7.	DNI design point	[W/m^2]	992	Calculated with clear sky model in HFLCAL
8.	Atmospheric transmittance	[]	Clear sky: $\eta_{atmo} = 0.99321 - 1.1176\text{E-}4 \cdot SLR + 1.97\text{E-}8 \cdot SLR^2$, for $SLR \leq 1000$ m. $\eta_{atmo} = e^{-1.106\text{E-}4 \cdot SLR}$, for $SLR > 1000$ m.	Standard clear sky model in HFLCAL. *SLR*: slant range
	Heliostat			
9.	Heliostat type/name	[]	Multi-facetted glass metal heliostat with 2-axes drive, pedestal mounted	Based on Abengoa Sanlúcar 120
10.	Net reflective area per heliostat	[m^2]	121.34	
11.	Facet reflecting surface	[m^2]	4.33	
12.	Aperture width	[m]	12.84	
13.	Aperture height	[m]	9.45	
14.	Height of Pylon	[m]	5.02	
15.	Number of facets	[-]	28 (4h x 7v)	
16.	Annual mean reflectivity	[%]	89.34	Product of reflectivity (94 %), mean cleanliness factor (96 %), and availability (99 %); (Giuliano, Puppe et al. 2017)
17.	Beam error	[mrad]	3.25	Sum for HFLCAL (slope error, tracking error, sun shape); (based on Balz, Göcke et al. 2016)
18.	Canting	[-]	On-axis	(Giuliano, Puppe et al. 2017)

No.	Item	Unit	Value	Comments
	Solar field – system definition			
19.	Field layout	[-]	Polar (Multi-tower)	
20.	Number of heliostats	[-]	1401	HFLCAL Optimization results
21.	Net field reflective area	[m²]	170 000	
22.	Optical efficiency of solar field @ DP	[%]	63.6	
23.	Optical efficiency of solar field annual	[%]	54.2	
	Solar tower			
24.	Type	[-]	Concrete	
25.	Number of towers	[-]	6	
26.	Solar multiple	[-]	2.5	
27.	Height of receiver center above ground	[m]	133.6	HFLCAL Optimization results
28.	Diameter	[m]	15	For shadow
	Solar receiver			
29.	Receiver type	[-]	CentRec©	
30.	Heat transfer medium (HTM)	[-]	Bauxite particles	
31.	Thermal power @DP	[MW_t]	96.23	
32.	Min/max thermal load	[%]	120 % / 10 %	
33.	HTM inlet temperature	[°C]	605.5	Input from D1.1
34.	HTM outlet temperature	[°C]	905	900 °C at PHX inlet
35.	Receiver model Parameter 1 Parameter 2 Parameter 3 Parameter 4	[] [-] [-] [-] [kW/(m² K)]	103 0.950 0.900 1.000 0.030	For field layout in HFLCAL: P1: Opt. Efficiency P2: Emissivity P3: Relative mean receiver temperature P4: Convective heat transfer coefficient

No.	Item	Unit	Value	Comments
36.	Aperture diameter	[m^2]	7.58	
37.	Mean flux on receiver aperture @ DP	[MW_t/m^2]	2.38	HFLCAL Optimization results
38.	Tilt angle	[°]	30.2	
39.	Receiver thermal efficiency @ DP	[%]	89.7	
40.	Receiver thermal efficiency annual	[%]	87.4	
	Power Block			
41.	Desing point net rating	[MW_e]	112.8	
42.	$T_{PHX,sCO2,out}$	[°C]	700	Project description
43.	$T_{PHX,sCO2,in}$	[°C]	558.1	Deliverable 1.1
44.	Power Block net efficiency	[%]	49.0	Partial cooling + RH cycle (Deliverable 1.1)
45.	Heat transfer coefficient Pa-PHX	[$W/(m^2\ K)$]	300	Needed for PHX cost correlation (Buck and Giuliano 2018)
	HFLCAL Cost models			
46.	5-digit code	[]	812	HFLCAL cost model
47.	DNI factor	[-]	0.7529	Ratio of annual DNI (meteo) over annual clear sky DNI
48.	Heliostat field	[EUR/m^2]	110	Including land and preparation
49.	Tower	[EUR]	1 767 767 EUR $e^{0.006931\ ath/m}$	*ath*: height of receiver center above ground
50.	Receiver (structural)	[EUR/m^2]	70 000	Cost per aperture area

No.	Item	Unit	Value	Comments
51.	Receiver (insulation)	[EUR/m^2]	1000 (1 + ($T_{Rec,out}$/K – 600)/400)	Cost per receiver insulated area (HFLCAL optimization result)
52.	Power block w/out PHX	[EUR/ $kW_{e,net}$]	1976	Including all indirect costs and contingencies for PB. Calculated with "sCO2euro_T_PHX" cost model in Deliverable 1.1.
53.	PHX	[EUR]	128122 * A_{HX}^0.66	Cost per heat transfer surface area (Buck and Giuliano 2018)
54.	Contingency	[%]	30	Estimate
55.	O & M	[%]	2.3	Annual O & M cost as fraction of CAPEX of heliostats, tower and receiver.
56.	Annuity	[%]	8.58	Discount: 7 %; Debt period: 25 a.